Journal of Materials Chemistry A

PAPER

View Article Online
View Journal | View Issue

Cite this: J. Mater. Chem. A, 2014, 2, 5427

An expanded isoindigo unit as a new building block for a conjugated polymer leading to high-performance solar cells†

Shugang Li,[b] Zhongcheng Yuan,[a] Jianyu Yuan,[a] Ping Deng,[b] Qing Zhang*[b] and Baoquan Sun*[a]

Received 19th December 2013
Accepted 16th January 2014

DOI: 10.1039/c3ta15291j

www.rsc.org/MaterialsA

Design and synthesis of novel monomers may create new opportunities for high performance semiconducting polymers. The synthetic modification of an isoindigo related building block based on rational design has been carried out in this study. An expanded isoindigo unit (IBTI) with 5,5′-divinyl-2,2′-bithiophene as a conjugated bridge has been successfully incorporated into a donor–acceptor conjugated polymer, **PBDT–IBTI**. The new polymer showed broad absorption and a large extinction coefficient in the visible region. The optical bandgap, HOMO and LUMO levels of this new polymer are 1.71 eV, −5.24 eV and −3.72 eV, respectively. The polymer solar cells based on **PBDT–IBTI** and (6,6)-phenyl-C61 butyric acid methyl ester ($PC_{61}BM$) blends achieved a PCE of 6.41%. This work has demonstrated that IBTI is a promising building block for organic photovoltaic (OPV) polymers. These findings have also revealed the versatility of oxindole as the basic building element for isoindigo-like conjugated monomers.

Introduction

Conjugated polymers have been extensively studied for applications in optoelectronic devices such as organic photovoltaics (OPVs) and organic field-effect transistors (OFETs).[1] Lactam based acceptors such as diketopyrrolopyrrole (DPP),[2] isoindigo (iI),[3] and benzodipyrrolidone[4] have been incorporated into many donor–acceptor polymers for OPV and OFET applications. Isoindigo processes a central carbon–carbon double bond which is conjugated with two oxindole rings to form an extended π-conjugated structure. Its importance as a building block for conjugated polymers has been evident from many recent studies of high-performance materials for OPV and OFET applications.[3,5–7]

Some recent studies suggested that the structure of isoindigo was slightly twisted because of steric repulsion between the protons on the phenyl rings and the carbonyl oxygens of the oxindoles (Fig. 1).[3a,b,6] This twist could reduce donor–acceptor interactions, the effective conjugation and could adversely affect the inter-chain stacking. To avoid the steric repulsion, several groups recently synthesized thienoisoindigo (TiI) as a monomer (Fig. 1).[6] The steric repulsion is relieved in TiI. Also, the short oxygen–sulfur distance in TiI can result in favorable Coulombic interactions between the oxygen atoms of the carbonyls and sulfur atoms of the thiophenes. This non-bonding interaction can enhance the coplanarity of the monomer.[6c] Many conjugated polymers based on TiI have been synthesized. The highest hole mobility of 0.28 $cm^2\ V^{-1}\ s^{-1}$ and the highest electron mobility of 0.03 $cm^2\ V^{-1}\ s^{-1}$ were achieved in ambipolar OFET devices based on those polymers.[6b] An OPV device study on TiI based polymers was also reported and a power conversion efficiency (PCE) of 4.27% was achieved.[6c] So far, most of the TiI based conjugated polymers show absorption expanding into the near infrared region and show a narrow bandgap. However, they also show very high HOMO energy levels. The high HOMO energy levels result in a very low open circuit voltage (V_{oc}) (about 0.5 V) in bulk heterojunction (BHJ) polymer solar cell devices.[6c]

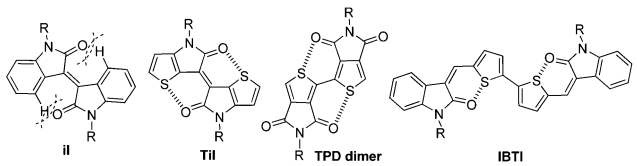

Fig. 1 Structures of isoindigo (iI), thienoisoindigo (TiI), thienopyrroledione (TPD dimer), and IBTI.

[a]Jiangsu Key Laboratory for Carbon-Based Functional Materials & Devices, Institute of Functional Nano & Soft Materials (FUNSOM), Soochow University, 199 Ren'ai Road, Suzhou 215123, China. E-mail: bqsun@suda.edu.cn

[b]Shanghai key lab of polymer and electrical insulation, School of Chemistry and Chemical Engineering, Shanghai Jiaotong University, 800 Dongchuan Road, Shanghai 200240, China. E-mail: qz14@sjtu.edu.cn

† Electronic supplementary information (ESI) available. See DOI: 10.1039/c3ta15291j

Herein, we report a novel polymer (**PBDT–IBTI**) based on an expanded isoindigo unit (IBTI) and benzo[1,2-*b*:4,5-*b*′]dithiophene (BDT) as the repeating units. Instead of a double bond as the bridge in isoindigo, the IBTI unit used 5,5′-divinyl-2,2′-bithiophene as the conjugated bridge to connect the two oxindole rings (Fig. 1). Therefore, the conjugated core was expended. The steric repulsion between the protons on the phenyl rings and the carbonyl oxygens of the oxindoles can be avoided in the new monomer. The four carbon atoms and the oxygen and sulfur atoms are positioned in space to form a spatial relation which resembled a six-member ring structure. The short oxygen–sulfur distance in the IBTI can also result in favorable Coulombic interactions between the carbonyl oxygen atoms of the oxindoles and the sulfur atoms of the thiophenes. Similar interactions in bisthienopyrroledione (TPD-dimer) and DPP were studied by DFT calculations and were confirmed by their X-ray crystal structure (Fig. 1).[8] The non-bonding interactions were considered important for coplanarity and conjugation.

Bis-oxindole with 5,5′-divinyl-2,2′-bithiophene as a bridge has been studied for small molecule OFET applications by Liu.[9] However, such a structure has never been incorporated into a donor–acceptor conjugated polymer for an OPV study. The compound reported by Liu was functionalized at the 5,5′ position. A recent study showed that the substitution pattern played a signification role on the photo-physical properties of the molecular isoindigo compound.[10] The 6,6′ substituted isoindigo derivatives showed greater extended π-conjugation compared to the 5,5′ substituted isoindigo derivatives because of the large contribution of the electronic transition dipole moment in the axis aligned with the 6,6′ carbons.[3a,10a] We chose to synthesize the bridged bis-oxindole building block (IBTI) with bromides positioned at the 6,6′ carbon position for achieving extended π-conjugation in the targeted polymer. The PSC device studies on the **PBDT–IBTI** polymer showed a high PCE of 6.41% and a high FF of 71%.

Experimental section

Materials and methods

All the chemicals were purchased from Sigma-Aldrich Chemical Co. and Sinopharm Chemical Reagent Co. Toluene was freshly distilled over sodium wire under a nitrogen atmosphere prior to use. Flash chromatography was carried out on silica gel (200–300 mesh). Nuclear magnetic resonance (NMR) spectra were recorded on a Mercury plus 400 MHz instrument. Gel permeation chromatography (GPC) analyses were carried out on a Shimadzu SIL-20A liquid chromatography instrument using tetrahydrofuran as the eluent with polystyrene as the standard. Thermogravimetric analyses (TGAs) were carried out on a TA instrument Q5000IR at a heating rate of 20 °C min^{-1} under nitrogen gas flow. Differential scanning calorimetry (DSC) studies were carried out with a Perkin Elmer Pyris 1 under nitrogen flow. The sample (about 5.0 mg in weight) was first heated to 300 °C and held for 2 min to remove the thermal history, followed by cooling at a rate of 10 °C min^{-1} to 20 °C and then heated at a rate of 10 °C min^{-1} to 300 °C. UV-vis spectra were recorded on a Perkin Elmer Lambda 20 UV-vis spectrophotometer. The absorption coefficient of the polymer in a chloroform solution was calculated according to the Beer–Lambert law. Cyclic voltammetry (CV) measurements were conducted on a CHI 600 electrochemical analyzer, with a three-electrode cell, under a nitrogen atmosphere, in a deoxygenated anhydrous acetonitrile solution of tetra-*n*-butylammoniumhexafluorophosphate (0.1 M), at a scan rate of 50 mV s^{-1}. A platinum disk electrode was used as the working electrode, a platinum wire was used as the counter electrode, and an Ag/Ag^{+} (0.01 M $AgNO_3$ in acetonitrile) electrode was used as the reference electrode. The polymer films were coated on the surface of the platinum disk electrode. The CV curves were calibrated with the ferrocene/ferrocenium (Fc/Fc^{+}) redox couple as an external standard which was measured under the same conditions before and after the measurement of the samples. Atomic force microscopy (AFM) images were obtained using a Multi Mode V microscope. Elemental analyses were performed at the Shanghai Institute of Organic Chemistry, Chinese Academy of Sciences.

Polymer solar cell fabrication and testing

PSC devices with the conventional structure of ITO/PEDOT:PSS(40 nm)/polymer:PCBM/LiF/Al were fabricated. Patterned ITO glass substrates were cleaned by ultrasonic treatment in an aqueous detergent solution, isopropyl alcohol and acetone sequentially. The organic residue was further removed by treating with UV-ozone for 20 min. A thin film of PEDOT:PSS (about 40 nm) was spin-coated onto the pre-cleaned ITO substrates and the substrates were dried at 150 °C for 10 min. A blend of the polymer and $PC_{61}BM$ was dissolved in a chosen solvent with or without DIO. The solution was filtered through a poly(tetrafluoroethylene) (PTFE) filter (0.45 μm) and was spin-coated at 1200 rpm for 40 s on top of the PEDOT:PSS layer. The samples were transferred into an evaporator. Lithium fluoride (0.6 nm) and aluminium (100 nm) layers were thermally deposited under a vacuum of 1.0×10^{-6} Torr through a shadow mask (active area 7.25 mm^2). The PSC devices with an inverted structure of ITO/ZnO/polymer:$PC_{61}BM/MoO_3$/Ag were fabricated as follows: a *ca.* 40 nm zinc oxide layer was obtained by spin-coating a sol–gel zinc oxide (ZnO) precursor solution onto the pre-cleaned indium tin oxide (ITO) substrates. The coated substrates were baked at 150 °C for 40 min in air and transferred into a nitrogen filled glove box. A chlorobenzene solution of the polymer (8 mg mL^{-1}) and $PC_{61}BM$ at different weight ratios with or without 1,8-diiodooctane (DIO) was spin coated on top of the zinc oxide layer. The samples were transferred into an evaporator and a MoO_3 layer (7 nm) and an Ag layer (80 nm) were thermally deposited under a vacuum of 1.0×10^{-6} Torr. The device area was restricted to 7.25 mm^2 by a shadow mask.

The PCEs were measured in a glove box directly after fabrication. The devices for the EQE measurements were encapsulated in the glove box and measured in air. A Newport 94023A solar simulator equipped with a 450 W xenon lamp and an air mass (AM) 1.5G filter was used to generate a simulated AM 1.5G

solar spectrum irradiation source. The irradiation intensity was 100 mW cm^{-2} calibrated by a Newport standard silicon solar cell 91150. A Newport monochromator 74125 and power meter 1918 with silicon detector 918D were used in the EQE measurements.

Procedure for synthesis of the monomer and polymer

The synthetic routes for the monomers and polymers are shown in Scheme 1. (*E*)-6,6′-Dibromo-1,1′-bis(2-octyldodecyloxy)-[3,3′-biindolinylidene]-2,2′-dione (il),[3b] 2,6-bis(trimethyltin)-4,8-di(2-ethylhexyl)-benzo[1,2-*b*:4,5-*b*′]-dithiophene (BDT),[11] 2,2′-bithiophene-5,5′-dicarbaldehyde,[12] and 6-bromooxindole (**1**)[3b] were synthesized according to literature procedures.

(3*Z*,3′*Z*)-3,3′-(2,2′-Bithiophene-5,5′-diylbis(methan-1-yl-1-ylidene))bis(6-bromoindolin-2-one) (2). To a suspension of 6-bromooxindole (4.40 g, 20.0 mmol) and 2,2′-bithiophene-5,5′-dicarbaldehyde (2.22 g, 10.0 mmol) in absolute alcohol (70 mL), piperidine (1.0 mL) was added. The mixture was refluxed for 24 h and a red precipitate formed. The reaction mixture was cooled to room temperature and was filtered. The solid material was washed with ethanol and was dried under vacuum to give the title compound (5.31 g, 87.0% yield). Due to its poor solubility, the product was used for the next step directly without further characterization.

(3*Z*,3′*Z*)-3,3′-(2,2′-Bithiophene-5,5′-diylbis(methan-1-yl-1-ylidene))bis(6-bromo-1-(2-octyldodecyloxy)indolin-2-one) (IBTI). Anhydrous potassium carbonate (3.85 g, 27.85 mmol) and **2** (3.40 g, 5.57 mmol) were dissolved in *N*,*N*-dimethylformamide (80 mL). The solution was heated at 120 °C for 1 h under nitrogen. 9-(Iodomethyl)nonadecane (6.83 g, 16.71 mmol) was added dropwise and the mixture was heated at 120 °C for 24 h. It was cooled to room temperature and was poured into water (300 mL). The mixture was extracted with dichloromethane. The combined organic layer was collected and was dried with anhydrous sodium sulfate. The solvent was removed under reduced pressure and the residue was purified by flash chromatography on silica gel with diethyl ether–hexane (1 : 10) as the eluent to give the title compound IBTI (2.70 g, 41.3% yield) as a dark red solid. ^{1}H NMR (400 MHz, $CDCl_3$, δ): 7.62 (d, J = 4.2 Hz, 2H), 7.60 (s, 2H), 7.43 (d, J = 4.2 Hz, 2H), 7.33 (dd, J = 8.1, 1.6 Hz, 2H), 7.16 (dd, J = 8.1, 1.5 Hz, 2H), 6.94 (d, J = 1.5 Hz, 2H), 3.64 (d, J = 7.5 Hz, 4H), 1.91 (m, 2H), 1.41–1.13 (m, 64H), 0.94–0.79 (m, 12H). ^{13}C NMR (100 MHz, $CDCl_3$, δ): 166.58, 145.05, 143.03, 138.58, 137.99, 128.11, 126.03, 125.00, 122.99, 122.13, 120.32, 119.93, 111.98, 44.77, 36.41, 32.13, 31.78, 30.22, 29.87, 29.81, 29.76, 29.57, 29.50, 26.66, 22.90, 14.34. Anal. calcd for $C_{66}H_{94}Br_2N_2O_2S_2$: C 67.67, H 8.09, N 2.39%; found: C 67.52, H 8.44, N 2.32%.

Polymer PBDT–IBTI. IBTI (0.35 g, 0.30 mmol), BDT (0.23 g, 0.30 mmol), $Pd_2(dba)_3$ (0.0055 g, 0.0060 mmol), P(*o*-tol)$_3$ (0.0073 g, 0.0240 mmol) and degassed toluene (10.0 mL) were added to a Schlenk tube. The solution was subjected to three cycles of evacuation and admission of nitrogen and was stirred at 90 °C for 4 h. After cooling to room temperature, the mixture was poured into methanol (100 mL) and was stirred for 2 h. A deep blue precipitate was collected by filtration. It was washed with methanol and the hexane in a Soxhlet extractor for 24 h each. It was extracted with hot chloroform in an extractor for 24 h. After removing the solvent, a dark blue solid with a metallic luster was collected (0.31 g, 70.1% yield). ^{1}H NMR (400 MHz, $CDCl_3$, δ): 8.1–6.5 (br, 14H), 4.4–3.5 (br, 8H), 2.0–0.5 (br, 108H). Anal. calcd for $(C_{92}H_{130}N_2O_4S_4)n$: C 75.88, H 9.00, N 1.92%; found: C 75.37, H 9.32, N 1.85%. GPC (THF): M_n = 43.5 kDa, M_w = 115.8 kDa, PDI = 2.67.

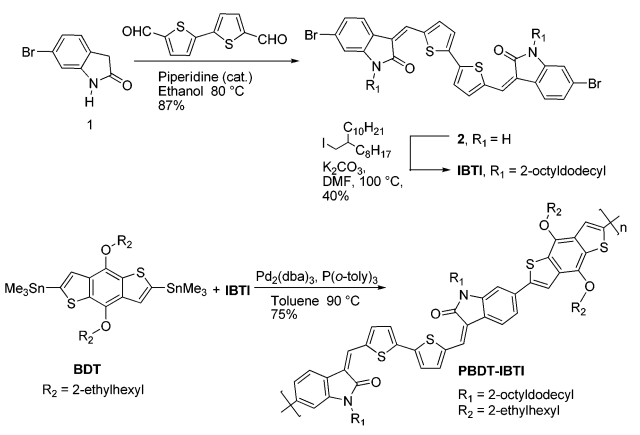

Scheme 1 Synthesis of monomer and polymer PBDT–IBTI.

Results and discussion

Synthesis and characterization

The key intermediate, **2**, was prepared by the Knoevenagel reaction of 6-bromooxindole and 2,2′-bithiophene-5,5-dicarbaldehyde in the presence of piperidine in absolute ethanol (Scheme 1). The stereoselectivity of this condensation reaction has been carefully studied using several different kinds of NMR techniques and a *Z*,*Z* configuration of the product have been firmly established in a recent paper by Liu.[9] The crude product, **2**, showed poor solubility in common solvents such as dichloromethane, acetone and ethyl ether. It was washed with methanol and was used directly in the next step. The large branched 2-octyldodecyl groups were chosen as side chains for improving the solubility. Compound **2** was *N*-alkylated to give the monomer IBTI. The polymer **PBDT–IBTI** was synthesized by Stille cross-coupling reaction with the monomer IBTI and 2,6-bis(trimethyltin)-4,8-di(2-ethylhexyloxy)benzo[1,2-*b*:4,5-*b*′]-dithiophene (BDT) at a 1 : 1 ratio in the presence of $Pd_2(dba)_3$ and P(*o*-tol)$_3$ as the catalyst and ligand (Scheme 1). The polymer was purified by precipitation in methanol and by washing with methanol and then hexane in a Soxhlet extractor for 24 h each. **PBDT–IBTI** was soluble in common organic solvents such as tetrahydrofuran, chloroform (CF) and chlorobenzene (CB) at room temperature. The number-average molecular weights (M_n) and the polydispersity index (PDI) of the polymers were determined by gel permeation chromatography (GPC) using polystyrene as the standard with tetrahydrofuran as the eluent. The polymer showed a relatively high M_n of 43.5 kDa and a PDI of 2.67.

Thermal properties

Thermogravimetric analyses of the polymer are exhibited in Fig. S4.† The **PBDT–IBTI** polymer revealed a decomposition temperature (T_d, at 5% weight loss) of 393 °C. However, it did not show any noticeable glass transition in the differential scanning calorimetry (DSC) analysis in the temperature range from 40 °C to 300 °C (Fig. S5†). These results indicate that **PBDT–IBTI** possesses a good thermal stability which is a prerequisite for device application.

Optical properties

The absorption spectra of IBTI, 6,6′-dibromodi(2-octyldodecyl) isoindigo (iI), and the **PBDT–IBTI** polymer in a CF solution are shown in Fig. 2a. The IBTI and iI monomers have same branched alkyl chains in this study. The spectra of the **PBDT–IBTI** thin film and the **PBDT–IBTI** dilute solution are displayed in Fig. 2b. The solution absorption spectrum of iI showed a high-energy band with a maximum at 402 nm ($\varepsilon = 3.03 \times 10^4$ M^{-1} cm^{-1}) and a much weaker low-energy band with a maximum at 503 nm. The solution absorption spectrum of the monomer IBTI displayed a single band with a maximum at 522 nm ($\varepsilon = 5.91 \times 10^4\ M^{-1}\ cm^{-1}$) and a shoulder at 552 nm. Due to the extended conjugation in IBTI, the IBTI spectrum was significantly red-shifted and had a much larger extinction coefficient at its peak compared to the iI spectrum. The solution absorption spectrum of the **PBDT–IBTI** polymer showed broad absorption from 475 to 700 nm with a maximum at 594 nm ($\varepsilon = 1.10 \times 10^5\ M^{-1}\ cm^{-1}$) and a shoulder at 641 nm. The absorption spectrum of the polymer thin-film was slightly red shifted (12 nm at maximum) compared with that of the solution spectrum. The thin-film spectrum showed a maximum at 606 nm with a shoulder at 657 nm. The optical bandgap was 1.71 eV calculated from the onset absorption (725 nm) from the thin-film spectrum. The new polymer showed broad absorption in the visible region and a large extinction coefficient. These are the required properties for conjugated polymers for high performance PSC applications.

Electrochemical properties

The cyclic voltammetry (CV) curve of the **PBDT–IBTI** polymer film is shown in Fig. 3a. The potentials were referenced to the ferrocene/ferrocenium redox couple (Fc/Fc^+). The redox potential of Fc/Fc^+ was assumed to have an absolute energy level of −4.8 eV in vacuum. The redox potential of Fc/Fc^+ was measured under the same conditions as the polymer samples and was located at 0.09 V relative to the Ag/Ag^+ electrode. The electrochemical potentials were converted to the corresponding energy levels by the following equations:[13]

$$E_{HOMO} = -(4.8 - E_{1/2,\ Fc,\ Fc+} + E_{ox,\ onset}) = -(4.71 + E_{ox,\ onset})\ eV$$

$$E_{LUMO} = -(4.8 - E_{1/2,\ Fc,\ Fc+} + E_{red,\ onset}) = -(4.71 + E_{red,\ onset})\ eV$$

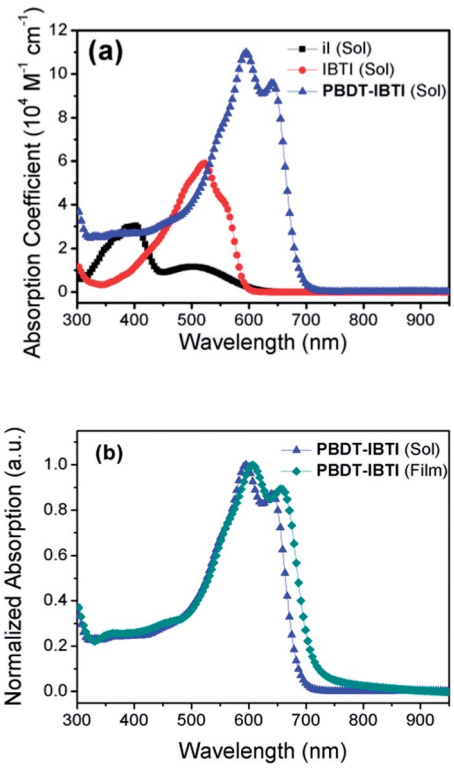

Fig. 2 UV-vis absorption spectra, (a) 6,6′-dibromodi(2-octyldodecyl) isoindigo (iI), IBTI monomer and **PBDT–IBTI** polymer in a chloroform solution; (b) **PBDT–IBTI** polymer in a chloroform solution and as a thin film.

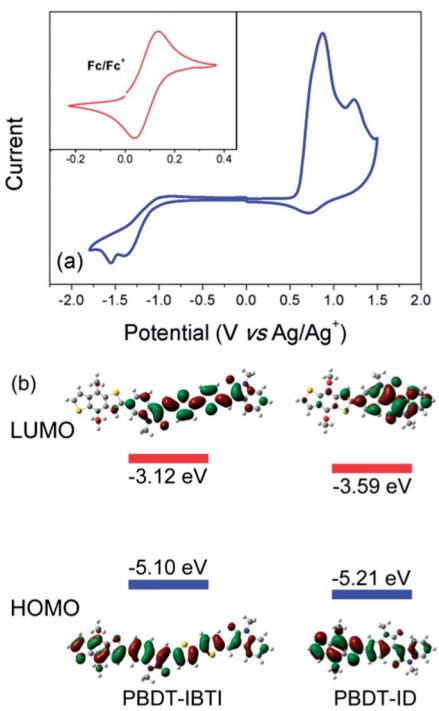

Fig. 3 Cyclic voltammograms (a) of **PBDT–IBTI** film in n-Bu_4NPF_6 solution (0.1 mol L^{-1} in acetonitrile) at a scan rate of 50 mV s^{-1}. Energy diagrams (b) showing theoretically calculated HOMO/LUMO energy levels as well as their topographical representations.

The CV curve showed the oxidation onset ($E_{ox,\ onset}$) at 0.53 V and the reduction onset ($E_{red,\ onset}$) at −0.99 V. The HOMO and LUMO energy levels were at −5.24 and −3.72 eV, respectively. The HOMO level is comparable to that of the isoindigo and bis(alkoxy)-substituted BDT copolymers (**PBDT–ID**).[5c] It is lower than those of the TiI-based polymers (about −5.0 eV).[6] The relatively low HOMO level is necessary for achieving a high open-circuit voltage (V_{oc}) in OPV devices and also improves the stability of the polymer by avoiding unintentional p-doping.[14] The energy levels of the new polymer resembled the ideal polymer which was described in the design rules for donor polymers for fullerene based BHJ solar cell devices.[15]

In order to gain further insights into the structural and electronic properties of polymers **PBDT–IBTI** and **PBDT–ID**, density functional theory (DFT) analysis was carried out at the B3LYP/6-31G** level of theory on model compounds representing the repeat units in the corresponding polymers (Fig. 3b). Their molecular orbital energy levels and orbital electron density plots were reported and compared with the experimental data. The theoretical HOMO/LUMO energies were found to be −5.10/−3.12 eV for **PBDT–IBTI** and −5.21/−3.59 eV for **PBDT–ID**, respectively. The HOMO wave function was more evenly delocalized over the whole polymer backbone in **PBDT–IBTI** than that in **PBDT–ID**, and the LUMO wave function was more effectively delocalized on the acceptor unit in **PBDT–IBTI** than in **PBDT–ID**. The HOMO wave function of **PBDT–IBTI** was favorable for transmission of the carrier.

Polymer photovoltaic device characteristics

The photovoltaic properties of the new polymer were investigated in PSC devices with a conventional structure of ITO/PEDOT:PSS/polymer:$PC_{61}BM$/LiF/Al. The devices were optimized by varying the weight ratios of the blend. The optimized weight ratio between the polymer and $PC_{61}BM$ was 1 : 2 (w/w). 1,8-Diiodooctane (DIO) was added as the processing additive to optimize the morphology of the active layer.[16] The current density–voltage (*J–V*) curves of the devices are presented in Fig. S7.† The device with PBDTT–FID:$PC_{61}BM$ (1 : 2, w/w) as the active layer processed with DIO (1%, v/v) from CB showed the best performance. It had a V_{oc} of 0.71 V, a J_{sc} of 9.40 mA cm^{-2}, a FF of 0.66 and a PCE of 3.0%.

Devices with inverted structures were also studied. The devices with a structure of ITO/ZnO/polymer:$PC_{61}BM$/MoO_3/Ag were fabricated and were tested under simulated illumination of air mass (AM) 1.5G (100 mW cm^{-2}). The weight ratios of **PBDT–IBTI** to $PC_{61}BM$ were varied from 1 : 1, 1 : 2 to 1 : 3. The electrical output characteristics were summarized in Table S1.† The best performances were from devices with a blend of **PBDT–IBTI** and $PC_{61}BM$ at 1 : 2 weight ratios. A PCE of 3.49% and a V_{oc} of 0.77 V can be achieved in devices based on such a blend. The device performances were limited by a low short-circuit current density (J_{sc}). Thermal annealing did not bring much improvement to the device performances. DIO was introduced to improve the morphology of the active layer. Addition of a small amount of DIO to a solution of the polymer and $PC_{61}BM$ before spin-coating significantly improved the solar cell performances.

The current density–voltage (*J–V*) curves are shown in Fig. 4a and the device performances are summarized in Table 1. The optimum DIO content was 2% (v/v). It resulted in a device with a V_{oc} of 0.77 V, a J_{sc} of 11.71 mA cm^{-2}, a FF of 71% and a PCE of 6.41%. The high J_{sc} of the devices resulted from the efficient light absorption and optimized morphology of the active layers. To confirm the accuracy of the measurement, the corresponding external quantum efficiency (EQE) of the solar cell device was measured under illumination of monochromatic light (Fig. 4b). The photo-response of the solar cell extended from 300 nm to 700 nm with a peak reaching nearly 60% around 600 nm. The EQE result was consistent with the UV-vis absorption spectrum of the **PBDT–IBTI**:$PC_{61}BM$ blend film.

The effect of the additive on the morphology was studied by atomic force microscopy (AFM). The AFM topography and phase images were measured on films which were spin-coated on top of ITO with a thin layer of zinc oxide from a blend of **PBDT–IBTI**:$PC_{61}BM$ (1 : 2, w/w) with or without DIO. DIO has been reported as an additive for the improvement of the morphology of the active layer.[14] The active layer processed with DIO [2% (v/v)] displayed an improved morphology compared with the one processed without DIO (Fig. 5). After addition of DIO, the big domains were broken into pieces, indicating good miscibility and large interface area between the donor and acceptor. The well-proportioned and interpenetrated morphology was achieved after addition of DIO. This ensured the efficient exciton separation and charge transport and resulted in the enhancement of the photocurrent (from 6.84 to 11.71 mA cm^{-2}) and PCE.

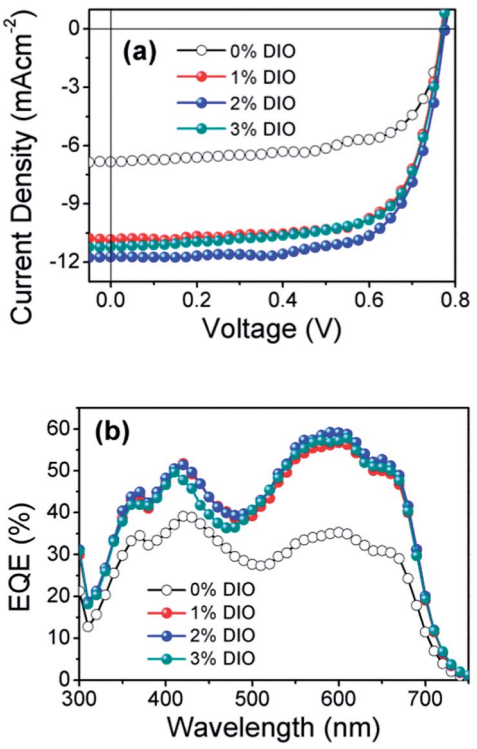

Fig. 4 (a) *J–V* curves and (b) EQEs for the conventional PSCs based on PBDT–IBTI:$PC_{61}BM$ (1 : 2, w/w) with different ratios of DIO in CB (v/v).

Table 1 The photovoltaic performance of the inverted PSCs based on **PBDT–IBTI**:$PC_{61}BM$ (1 : 2, w/w) (8 mg mL^{-1}) with different ratios of DIO in CB (v/v)

DIO[a] (v/v)	V_{oc} (V)	J_{sc} (mA cm^{-2})	FF	PCE (%)
0% DIO	0.77	6.84	0.66	3.49
1% DIO	0.76	10.81	0.71	5.89
2% DIO	0.77	11.71	0.71	6.41
3% DIO	0.76	11.07	0.72	6.09

[a] DIO content in chlorobenzene.

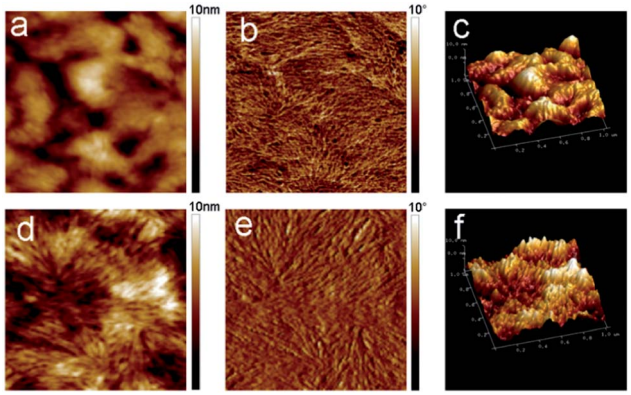

Fig. 5 AFM images of active layers processed from **PBDT–IBTI**:$PC_{61}BM$ (1 : 2, w/w) blend film: height images (a and d), phase images (b and e), and topography images (c and f), without DIO (upper row) and with 2% DIO (lower row). All images are 1 × 1 μm.

Conclusions

Synthetic modification of isoindigo related building blocks based on rational design has been carried out in this study. An expanded isoindigo unit with 5,5′-divinyl-2,2′-bithiophene as the conjugated bridge has been successfully incorporated into a donor–acceptor conjugated polymer for the first time. The steric repulsion has been avoided and favorable oxygen–sulfur non-bonding interactions have been introduced into the building block. The new polymer, **PBDT–IBTI**, showed broad absorption in the visible region, a large extinction coefficient and a relatively low HOMO energy level. The optical bandgap and HOMO and LUMO levels of this polymer are 1.71 eV, −5.24 eV and −3.72 eV, respectively. Polymer solar cells based on **PBDT–IBTI**:$PC_{61}BM$ blends as the active layer achieved a PCE of 6.41%. This work has demonstrated that IBTI is a promising building block for OPV polymers. Furthermore, this work has shown the versatility of oxindole as a basic building element for expanded isoindigo-like conjugated monomers.

Acknowledgements

This work was supported by the National Natural Science Foundation of China (NSFC grant nos 21174084, 21274087), by the National Basic Research Program of China (973 Program) (2012CB932402), and by the Doctoral Fund of the Ministry of Education of China (grant no. 20120073110032).

Notes and references

1 (*a*) G. Yu, J. Gao, J. C. Hummelen, F. Wudl and A. J. Heeger, *Science*, 1995, **270**, 1789; (*b*) S. Günes, H. Neugebauer and N. S. Sariciftci, *Chem. Rev.*, 2007, **107**, 1324; (*c*) A. Facchetti, *Chem. Mater.*, 2011, **23**, 733; (*d*) J. Hou and L. Huo, *Polym. Chem.*, 2011, **2**, 2453; (*e*) S. Steinberger, A. Mishra, E. Reinold, E. Mena-Osteritz, H. Müller, C. Uhrich, M. Pfeiffer and P. Bäuerle, *J. Mater. Chem.*, 2012, **22**, 2701; (*f*) G. C. Welch, L. A. Perez, C. V. Hoven, Y. Zhang, X.-D. Dang, A. Sharenko, M. F. Toney, E. J. Kramer, T.-Q. Nguyen and G. C. Bazan, *J. Mater. Chem.*, 2011, **21**, 12700.

2 (*a*) J. M. Jiang, M. C. Yuan, K. Dinakaran, A. Hariharan and K.-H. Wei, *J. Mater. Chem. A*, 2013, **1**, 4415; (*b*) L. Bürgi, M. Turbiez, R. Pfeiffer, F. Bienewald, H.-J. Kirner and C. Winnewisser, *Adv. Mater.*, 2008, **20**, 2217.

3 (*a*) R. Stalder, J. Mei, K. R. Graham, L. A. Estrada and J. R. Reynolds, *Chem. Mater.*, 2014, **26**, 664; (*b*) P. Deng and Q. Zhang, *Polym. Chem.*, 2013, DOI: 10.1039/c3py01598j; (*c*) T. Lei, J.-H. Dou and J. Pei, *Adv. Mater.*, 2012, **24**, 6457; (*d*) T. Lei, Y. Cao, X. Zhou, Y. Peng, J. Bian and J. Pei, *Chem. Mater.*, 2012, **24**, 1762; (*e*) C. Wang, B. Zhao, Z. Cao, P. Shen, Z. Tan, X. Li and S. Tan, *Chem. Commun.*, 2013, **49**, 3857; (*f*) Z. Ma, W. Sun, S. Himmelberger, K. Vandewal, Z. Tang, J. Bergqvist, A. Salleo, J. W. Andreasen, O. Inganäs, M. R. Andersson, C. Müller, F. Zhang and E. Wang, *Energy Environ. Sci.*, 2014, **7**, 361.

4 (*a*) W. B. Cui, J. Yuen and F. Wudl, *Macromolecules*, 2011, **44**, 7869; (*b*) P. Deng, L. Liu, S. D. Ren, H. X. Li and Q. Zhang, *Chem. Commun.*, 2012, **48**, 6960; (*c*) J. W. Rumer, M. Levick, S.-Y. Dai, S. Rossbauer, Z. Huang, L. Biniek, T. D. Anthopoulos, J. R. Durrant, D. J. Procter and I. McCulloch, *Chem. Commun.*, 2013, **49**, 4465.

5 (*a*) T. Lei, J.-H. Dou, Z.-J. Ma, C.-J. Liu, J.-Y. Wang and J. Pei, *Chem. Sci.*, 2013, **4**, 2447; (*b*) Y. Deng, J. Liu, J. Wang, L. Liu, W. Li, H. Tian, X. Zhang, Z. Xie, Y. Geng and F. Wang, *Adv. Mater.*, 2014, **26**, 471; (*c*) G. Zhang, Y. Fu, Z. Xie and Q. Zhang, *Macromolecules*, 2011, **44**, 1414; (*d*) E. Wang, Z. Ma, Z. Zhang, K. Vandewal, P. Henriksson, O. Inganäs, F. Zhang and M. R. Andersson, *J. Am. Chem. Soc.*, 2011, **133**, 14244; (*e*) T. Lei, Y. Cao, Y. L. Fan, C.-J. Liu, S.-C. Yuan and J. Pei, *J. Am. Chem. Soc.*, 2011, **133**, 6099.

6 (*a*) R. S. Ashraf, A. J. Kronemeijer, D. I. James, H. Sirringhaus and I. McCulloch, *Chem. Commun.*, 2012, **48**, 3939; (*b*) G. K. Dutta, A.-R. Han, J. Lee, Y. Kim, J. H. Oh and C. Yang, *Adv. Funct. Mater.*, 2013, **23**, 5317; (*c*) M. S. Chen, J. R. Niskala, D. A. Unruh, C. K. Chu, O. P. Lee and J. M. J. Fréchet, *Chem. Mater.*, 2013, **25**, 4088.

7 (*a*) T. Lei, J.-H. Dou, X.-Y. Cao, J.-Y. Wang and J. Pei, *J. Am. Chem. Soc.*, 2013, **135**, 12168; (*b*) Z. Yan, B. Sun and Y. Li, *Chem. Commun.*, 2013, **49**, 3790; (*c*) X. Zhang, Z. Lu, L. Ye,

C. Zhan, J. Hou, S. Zhang, B. Jiang, Y. Zhao, J. Huang, S. Zhang, Y. Liu, Q. Shi, Y. Liu and J. Yao, *Adv. Mater.*, 2013, **25**, 5791.

8 (*a*) Z. Chen, M. J. Lee, R. S. Ashraf, Y. Gu, S. Albert-Seifried, M. M. Nielsen, B. Schroeder, T. D. Anthopoulos, M. Heeney, I. McCulloch and H. Sirringhaus, *Adv. Mater.*, 2012, **24**, 647; (*b*) X. Guo, N. Zhou, S. J. Lou, J. W. Hennek, R. P. Ortiz, M. R. Butler, P.-L. T. Boudreault, J. Strzalka, P.-O. Morin, M. Leclerc, J. T. L. Navarrete, M. A. Ratner, L. X. Chen, R. P. H. Chang, A. Facchetti and T. J. Marks, *J. Am. Chem. Soc.*, 2012, **134**, 18427.

9 T. Wu, C. Yu, Y. Guo, H. Liu, G. Yu, Y. Fang and Y. Liu, *J. Phys. Chem. C*, 2012, **116**, 22655.

10 (*a*) L. A. Estrada, R. Stalder, K. A. Abboud, C. Risko, J.-L. Brédas and J. R. Reynolds, *Macromolecules*, 2013, **46**, 8832; (*b*) L. A. Estrada and D. C. Neckers, *Org. Lett.*, 2011, **13**, 3304.

11 J. Hou, M. Park, S. Zhang, Y. Yao, L. Chen, J. Li and Y. Yang, *Macromolecules*, 2008, **41**, 6012.

12 R. Chen, X. Yang, H. Tian, X. Wang, A. Hagfeldt and L. Sun, *Chem. Mater.*, 2007, **19**, 4007.

13 Y. Li, Y. Cao, J. Gao, D. Wang, G. Yu and A. J. Heeger, *Synth. Met.*, 1999, **99**, 243.

14 J. K. Lee, W. L. Ma, C. J. Brabec, J. Yuen, J. S. Moon, J. Y. Kim, K. Lee, G. C. Bazan and A. J. Heeger, *J. Am. Chem. Soc.*, 2008, **130**, 3619.

15 (*a*) N. Blouin, A. Michaud, D. Gendron, S. Wakim, E. Blair, R. Neagu-Plesu, M. Belletete, G. Durocher, Y. Tao and M. Leclerc, *J. Am. Chem. Soc.*, 2008, **130**, 732; (*b*) M. C. Scharber, D. Muhlbacher, M. Koppe, P. Denk, C. Waldauf, A. J. Heeger and C. J. Brabec, *Adv. Mater.*, 2006, **18**, 789.

16 J. Peet, J. Y. Kim, N. E. Coates, W. L. Ma, D. Moses, A. J. Heeger and G. C. Bazan, *Nat. Mater.*, 2007, **6**, 497.